Multivalent Probes in Molecular Imaging

Bohmer, Verena I.; Szymanski, Wiktor; Feringa, Ben L.; Elsinga, Philip H.

Published in:
TRENDS IN MOLECULAR MEDICINE

DOI:
10.1016/j.molmed.2020.12.006

Publication date:
2021

Trends in
Molecular Medicine

CellPress

Review

Multivalent Probes in Molecular Imaging: Reality or Future?

Verena I. Böhmer,[1,2] Wiktor Szymanski,[2,3] Ben L. Feringa,[2] and Philip H. Elsinga[1,*]

The rapidly developing field of molecular medical imaging focuses on specific visualization of (patho)physiological processes through the application of imaging agents (IAs) in multiple clinical modalities. Although our understanding of the principles underlying efficient IAs design has increased tremendously, many IAs still show poor *in vivo* imaging performance because of low binding affinity and/or specificity. These limitations can be addressed by taking advantage of multivalency, in which multiple copies of a ligand are employed to strengthen the interaction. We critically address specific challenges associated with the application of multivalent compounds in molecular imaging, and we give directions for a stepwise approach to the design of multivalent imaging probes to improve their target binding and pharmacokinetics (PK) for improved diagnostic potential.

Highlights

Multivalency is a powerful tool to increase the binding affinity of ligands, and this can greatly enhance image performance in molecular imaging modalities.

Successful translation of multivalent molecular imaging agents (MMIAs) requires careful design of the core and selection of the best possible ligand–linker combination through understanding their binding properties.

Rational design of MMIAs often neglects several key aspects, including the choice of the multivalent scaffold, its ligand-availability, and its dependencies on physiological conditions and biological barriers.

Achieving high imaging performance of MMIAs imposes additional considerations compared with monovalent molecules because of their size, steric factors, and pharmacokinetic properties.

Challenges and Applications of Molecular Imaging in Medicine

Medical imaging enables the visualization of anatomical structures and physiological processes for diagnostic purposes [1,2], and is commonly subcategorized into structural, functional, and molecular imaging [3]. Molecular imaging reveals diagnostically relevant biochemical information [4,5] at cellular and molecular levels *in vivo* [6,7]. Therefore, in addition to diagnostic applications, it also empowers drug development because it allows the study of drug pharmacokinetics (PK) at sub-toxic/therapeutic doses [4]. Typical molecular imaging techniques include positron emission tomography (PET), single-photon emission computed tomography (SPECT), optical imaging (OI), and, increasingly, magnetic resonance imaging (MRI) [5,8], although the use of MRI is still restricted because of limited sensitivity [8,9]. All molecular imaging techniques described here rely on the application of molecular imaging agents (IAs) that selectively target (disease-specific) biomarkers such as receptors, enzymes, transporters, physiological processes, or cellular uptake mechanisms [8], and can even participate in cell signaling cascades [10,11].

The developmental processes for molecular IAs and pharmaceuticals are relatively similar [12]. However, unlike pharmaceuticals, the concentration of IAs required for informative image acquisition is too low to evoke any pharmacological effect. An important property of IAs is their **binding potential** (**BP**, see Glossary) at the target site that ensures adequate accumulation and results in a diagnostically informative image with sufficient contrast. BP is defined as the ratio of the **target density** (B_{max}) to the **equilibrium dissociation constant** (K_d) of the IA, which is the inverse of the binding affinity of IAs [13–15] (Box 1 summarizes the relevant factors for obtaining a good molecular IA).

Many IAs suffer from a binding affinity that is too low (i.e., a high K_d), which in combination with a low B_{max} results in insufficient accumulation of IAs in the desired target tissue to provide a high-contrast image [16] leading to a low signal-to-noise ratio [8]. One way to improve the binding affinity is by utilizing the multivalency effect. Multivalent IAs are of specific interest for pathologies (oncology, cardiovascular disease, infection) where novel targets with low expression levels are linked to specific treatment options. These multivalent IAs are crucial for multivalency-based

[1]Department of Nuclear Medicine and Molecular Imaging, Medical Imaging Center, University Medical Center Groningen, Hanzeplein 1, 9713, GZ, Groningen, The Netherlands
[2]Stratingh Institute for Chemistry, University of Groningen, Nijenborgh 4, 9747, AF, Groningen, The Netherlands
[3]Department of Radiology, Medical Imaging Center, University Medical Center Groningen, Hanzeplein 1, 9713, GZ, Groningen, The Netherlands

*Correspondence:
p.h.elsinga@umcg.nl (P.H. Elsinga).

drug development (e.g., nanomedicine) owing to their enhanced targeting selectivity. Because multivalent medical IAs (MMIAs) can generate high-contrast images, they can help in selecting the right therapy for the right patient at the right time with the right dose. However, using multivalency for medical imaging purposes faces several obstacles because MMIAs can have usual behaviors. We provide an overview of challenges in the field of MMIAs with respect to their target binding and PK properties. Based on these challenges, we formulate a stepwise approach for the design of MMIAs to improve their medical imaging properties.

How Multivalency Increases the BP of IAs

Multivalency is observed in Nature, where multiple copies of ligands are employed in one molecule to strengthen weak interactions [17]. The everyday life example of the multivalency concept is found in the form of Velcro, which was inspired by the burrs of the burdock plant that easily adhere to textiles [18]. Intriguingly, the same principle operates in the human body in the form of the antibody IgM that contains five copies of the monomer [19]. The strength of multiple interactions achieved by these multivalent complexes is a cumulative effect of all possible binding interactions and is defined as avidity [20]. The effect of multivalency is based on the decrease of the dissociation constant (K_d^{multi}) [17] as a result of a high local concentration of the ligand [21] (described in detail in Box 2).

Application of the concept of multivalency to molecular imaging can result in improved image contrast owing to a higher BP because multivalency leads to a higher binding avidity, resulting in a low K_d^{multi}. To some extent it can also increase the specificity of interactions with the target [22–24]. However, MMIAs are, despite many efforts, not yet used routinely in the clinic. This is mainly due to several knowledge gaps with respect to their avidity, PK, and other properties that are elaborated upon in the following sections.

Interactions of Multivalent Constructs with Their Molecular Targets, and Consequences for the Design of MMIAs

The interaction between multivalent ligand and target is based on the binding affinity [25]. In the case of multivalent binding, the effective binding can be enhanced by one or more of the five distinguishable 'multivalency effects'. These are (i) the chelate effect, (ii) the clustering effect, (iii) steric stabilization, (iv) subsite binding, and (v) the statistical effect (Figure 1). These different effects are strongly related to the target. The chelation effect usually occurs when oligomeric receptors are

Glossary

Binding potential (BP): the ratio of the target concentration (B_{max}) to the equilibrium dissociation constant (K_d) of the IA: BP = B_{max}:K_d

Boltzmann constant (k_B): $k_B = 1.38065 \times 10^{-23}$ J.K^{-1}

Degeneracy coefficient (Ω_1): prefactor that includes the fact that a multivalent molecule has Ω_1 distinguishable interactions and not only one.

Equilibrium dissociation constant (K_d): defined as C(target) * C(ligand) / C (ligand-target complex) [t) × (ligand] (ligand–t).

Half-life ($t_{1/2}$): a measure of radioactivity – the time required for half of the radioactivity to decay.

Partition coefficient (log*P*): expresses the lipophilicity of molecules. The most common method for determining log*P* is by the water/*n*-octanol distribution method at room temperature, in which the concentration (*C*) of the molecule is determined in each phase, and log*P* = log($C_{octanol}$/C_{water}).

Target density (B_{max}): defined as moles of the target receptor per gram of tissue.

Vandetanib: an inhibitor of tumor angiogenesis and tumor cell proliferation.

Box 1. Achieving High Binding Affinity of Molecular IAs

Medical imaging is used to obtain a better understanding of the malfunctioning of the human body which helps the physician to provide the correct diagnosis. Hence, the image obtained must have adequate contrast to provide a reliable source of information. A rule of thumb for PET/SPECT radiopharmaceuticals is to achieve a BP of ≥4 [13]. The BP (calculated as B_{max}:K_d) of IAs can be adjusted by the affinity of the IA itself: first and foremost this is determined by the target-specific binding ligand, which can be a small molecule, an antibody, or a peptide analog [8,74], that enables the required specific (molecular) interactions. The choice of ligand depends on the target and whether the desired information is related to, for example, receptor binding, metabolism, or active transporters [13]. Ligands are coupled to an imaging tag, for example, a fluorophore (optical imaging), a paramagnetic metal complex (MRI), or a radionuclide (PET, SPECT) [8,29], to enable the IA readout. In some cases, IAs require a linker between the ligand and the imaging tag to facilitate ligand–target interactions [29,75] (Figure I).

B_{max} can be considered to be constant for a particular type of tissue of a given patient during image acquisition, and lies typically in the nano- to even picomolar concentration range [8]. At the same time, the change in the patient-specific B_{max} over time can itself be an important pathological biomarker, as in the case of the translocator protein (TSPO) in the central nervous system that can be visualized using [^{11}C]PK11195 or [^{11}C]PBR28 [76]. Therefore, IAs must be constructed in such a way that they exhibit high binding affinities (i.e., low K_d values) for their target to achieve a BP of >4. High tissue accumulation of IAs requires moderate dissociation rate constants (K_{off}) [75,77] to enable a long residence time in the targeted tissue and fast wash-out of unbound IAs. Therefore, it is important to understand the interaction between ligand and target because these interactions can be reversible [78], irreversible [77], or the ligands can even be internalized [77].

IAs need to show a high stability *in vivo*, especially because any metabolite coupled to the imaging tag forms a confounding factor in obtaining a diagnostically useful image [13,75]. Furthermore, IAs should exhibit favorable degree of lipophilicity [13] to reach the desired targets, which might involve crossing the BBB – for which the IA must have a **partition coefficient (log*P*)** of 1.5–4 [13].

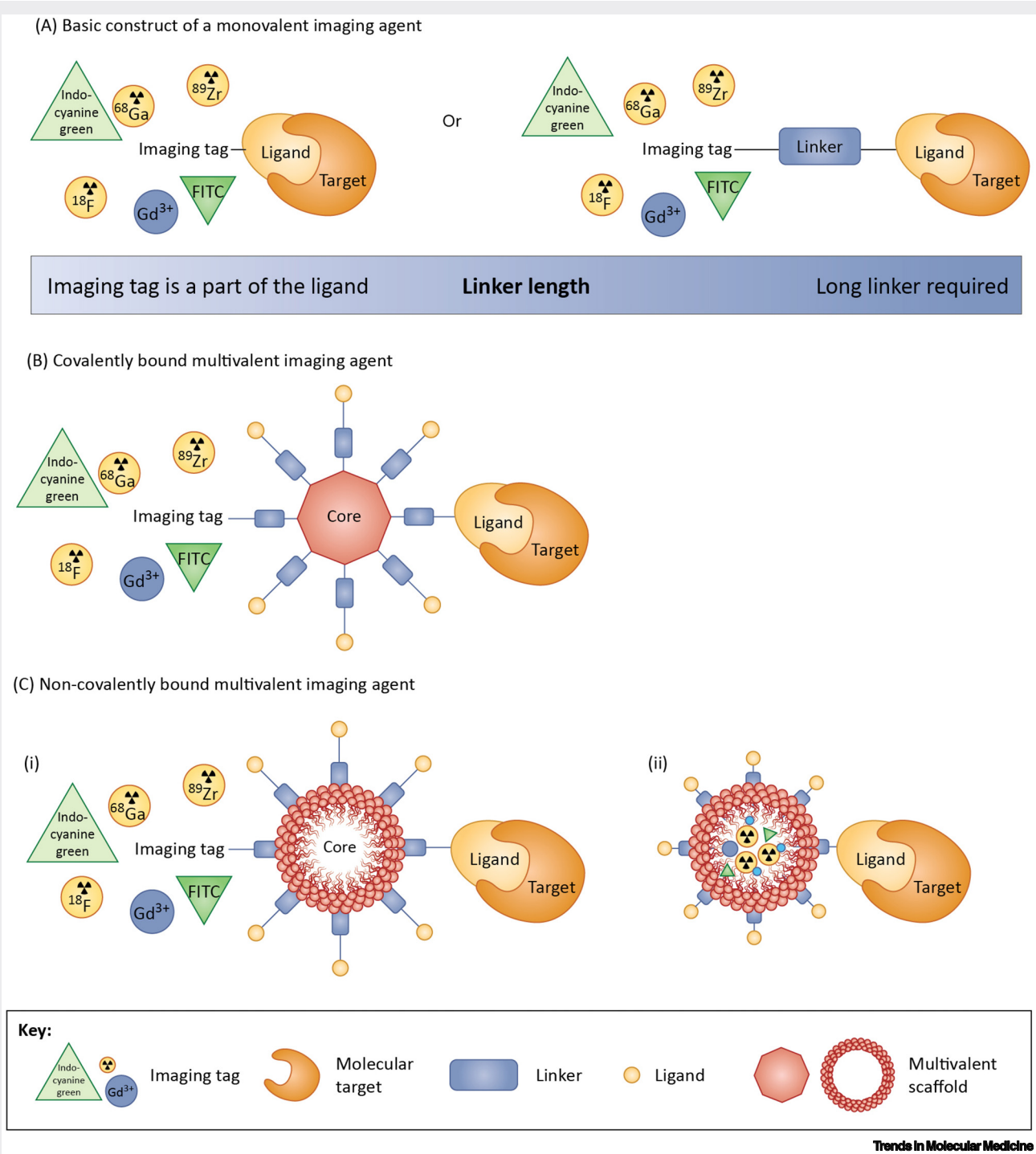

Figure I. Composition of Mono- and Multivalent Imaging Agents (IAs). (A) A monovalent IA composed of a target-binding ligand, optionally a linker, and an imaging tag. (B,C) A multivalent IA consists of an imaging tag attached through a linker to the core, which is functionalized with multiple ligands. (B) The core can be covalently assembled based on linear or branched polymers, dendrimers, or nanoparticles. (C) The core can be non-covalently bound, as exemplified by (i) self-assembly into a liposome that has a random distribution of ligands and imaging tags on the surface, and by (ii) liposome-based imaging agents that carry the imaging agents in their lumen and release their cargo after cellular uptake. Abbreviation: FITC, fluorescein isothiocyanate.

targeted, such as G protein-coupled receptors (e.g., dopamine receptors) that are known to form several homo- or heteromeric oligoreceptors [26]. The clustering effect occurs for non-oligomeric receptors that are able to freely move within the lipid bilayer [27], such as the lectin concanavalin A that binds to several manno- and glyco-pyranosides [28]. Steric stabilization describes competitive binding at the target site, for example, between a bound inhibitor and an unbound agonist [27]. Subsite binding describes the situation in which the multivalent ligand binds to an additional subsite at the target of a mono- or oligomeric receptor [27], which typically occurs in enzymes [29]. Lastly, the statistical effect describes the avidity improvement by a statistically increased local ligand concentration [27].

These multivalency effects occur in addition to the key interactions between ligand and target. This results in several functional and synthetic challenges for MMIAs that often counteract the predicted improvement of the BP of MMIAs. One reason for the discrepancy between the predicted and actual BP may be the behavior of the target upon multivalent binding because MMIA structure can have an influence on the behavior of the target. Therefore, one must choose which of the two different types of MMIAs – covalent and non-covalent – would best support the underlying multivalency effect by their geometry and ligand concentration. Covalent MMIAs are composed of a multivalent scaffold that is connected to a ligand, often through a linker [30,31] (Box 1). Non-covalent MMIAs are based on self-assembly to generate a liposome or micelle structure

Box 2. Thermodynamics of Multivalent Binding

The positive influence of multivalency on protein and cell interactions was first reported in 1979 when it was found that multivalency can increase the specificity of antibodies, depending on the equilibrium and rate constants of the different binding events [79]. The same phenomenon is true for receptor–ligand and cell–cell interactions [79]. Because this improvement is based on the free energies of the binding between receptors and ligand, the phenomenon can be clarified by examining the thermodynamics of multivalent molecules binding to their target. The Gibbs free energy (ΔG°) of monovalent binding is defined as in [80]:

$$\Delta G^\circ_{monovalent} = \Delta H^\circ - T\Delta S^\circ \quad [I]$$

The Gibbs free energy for the binding of a multivalent molecule depends on the valency of the compound (n) of each possible monovalent binding, as well as on the correction for tethering effects. This results in an overall higher Gibbs free energy [29,80]:

$$\Delta G^\circ_{multimer} = n\Delta G^\circ_{monovalent} - \Delta G^\circ_{interaction} \quad [II]$$

However, the standard free energy of multimers is not only determined by the valency of the multivalent molecule (n) but also by the number of binding sites (m) on the cell surface and the number of ligand–target bonds formed (i). This dependency is thermodynamically combined in the degeneracy coefficient Ω_i that quantifies all possible ligand–target interactions in multivalent systems and is dependent on the spatial arrangement and rigidity/flexibility of both counterparts (Figure I) [42]. Furthermore, the multivalent free energy must consider the inter- and intramolecular interactions (ΔG°_{inter} and ΔG°_{intra}, respectively) [27,80] together with the **Boltzmann constant** (k_B) and the temperature T in the following equation:

$$\Delta G^\circ_{multimer} = \Delta G^\circ_{inter} + (n-1)\Delta G^\circ_{intra} - k_B T \ \ln \Omega_i \quad [III]$$

Multivalency directly leads to increased entropy owing to the higher degeneracy coefficient Ω_i for multivalent constructs than for monovalent ($n = m = 1$) interactions. This is specified as the avidity entropy $\Delta S^\circ_{avidity}$ [81]:

$$\Delta S^\circ_{aviditiy} = k_B \ \ln \Omega_i \quad [IV]$$

The degeneracy coefficient Ω_i also influences the avidity of the system and, together with the equilibrium constants of inter- (K_{inter}) and intramolecular (K_{intra}) interactions, the generic avidity association constant ($K_A^{Avidity}$) can be calculated as follows [27,42]:

$$K_A^{Avidity} = \Omega_1 K_{inter} + \Omega_2 K_{inter} K_{intra_2} + \Omega_3 K_{inter} K_{intra_3}{}^2 + \ldots + \Omega_i K_{inter} K_{intra_i}{}^{i-1} \quad [V]$$

In Equation V the intramolecular interactions K_{intra} is categorized into '2, 3, … , i' because these variables indicate that cooperative effects influence subsequent binding. If cooperativity is negligible, K_{intra} is a constant – as commonly assumed in drug delivery systems [27,81]. $K_A^{Avidity}$ directly lead to the so-called enhancement factor (β) that describes the ratio between the multivalent association constant and the monovalent association constant [29]. Furthermore, it was shown that the multivalency effect leads to improved selectivity particularly for multivalent compounds with low B_{max} (low m number) [82].

Overall, the energy of a multivalent interaction is not simply the sum of the energies of monovalent interactions. Instead, the thermodynamics of multivalent binding is multidimensional because several factors play a role, including the valency of the MMIA, the number of binding sites it can interact with, and the number of bonds formed.

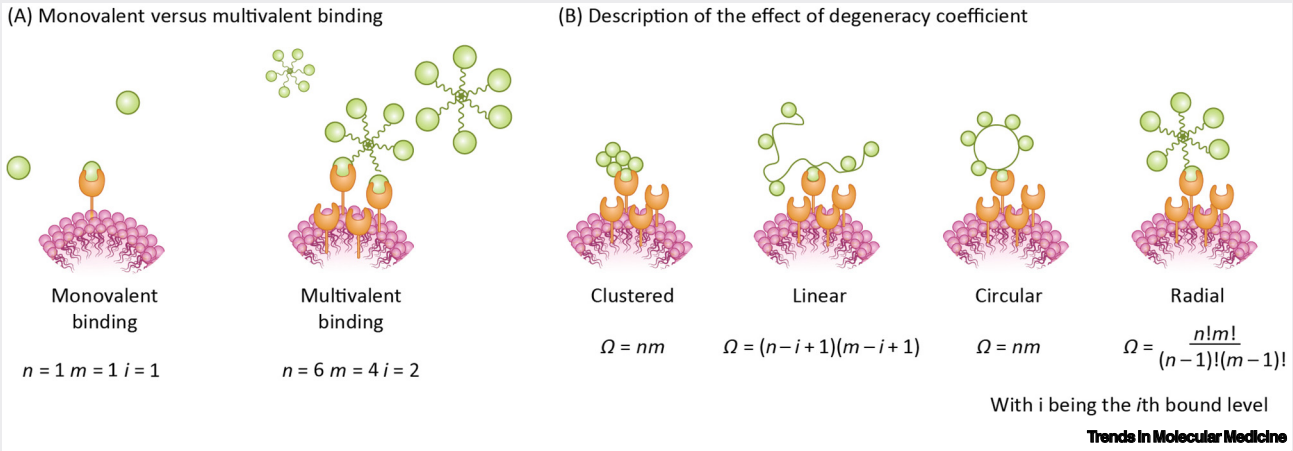

Figure I. Illustration of the Effect of Multivalency on the Thermodynamics of Multivalent Binding. Whereas monovalent binding is based on a single ligand that binds to its target, multivalent binding is created by a compound consisting of several ligands on the surface of a core molecule. The number of ligands and the core structure (linear, circular, or radial) strongly influence the degeneracy coefficient, which is a measure of energy states of the possible binding interactions. Figure modified, with permission, from [28].

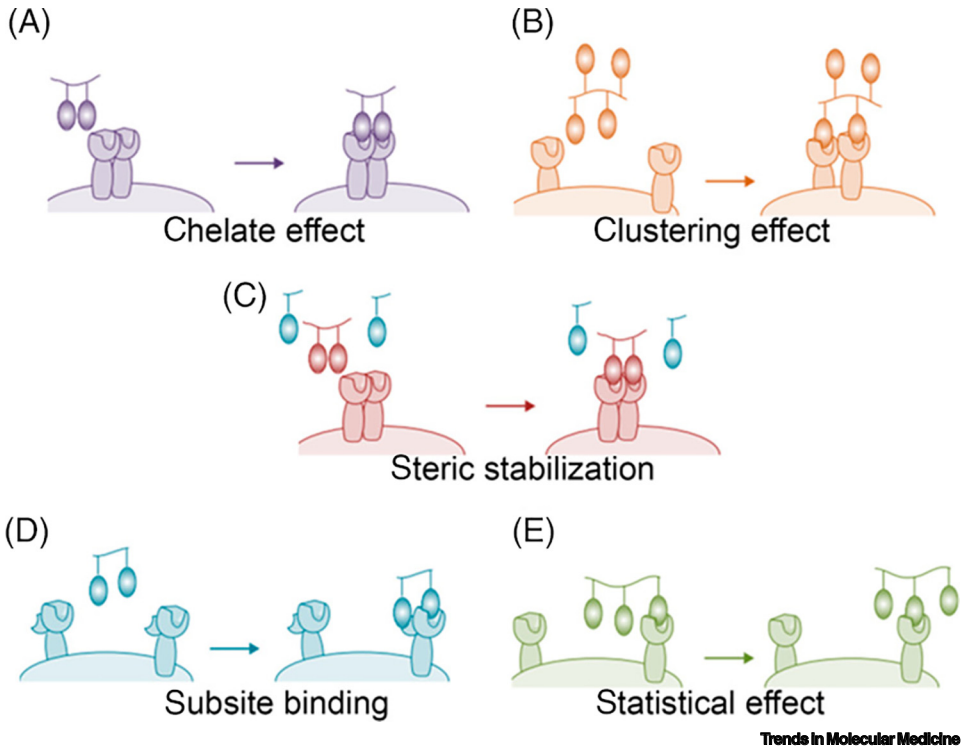

Figure 1. The Five Distinct Multivalency Effects. (A) Chelate effect: simultaneous ligand–target interaction at multiple binding sites. (B) Clustering effect: target sites cluster together on the cell surface. (C) Steric stabilization: the multivalent compound prevents another compound from binding to the target site. (D) Subsite binding: several binding sites on one target interact with the ligands. (E) Statistical effect: a higher local concentration increases the apparent affinity [11,28]. Figure reproduced, with permission, from [34].

that either comprises the IA or the IA is located inside the liposomal core. The ligands and imaging tags can be coupled to the linker, exactly as for covalent MMIAs, or the imaging tags can be incorporated into the liposomal lumen space [30,32].

Because multivalency effects play an important role in designing a successful MMIAs, the focus needs to be on maximizing the avidity entropy by optimizing the **degeneracy coefficient** (Ω_i). This can be achieved by adjusting the intricate interrelationship between ligand, multivalent scaffold, and linker length (and not only by increasing the valency of ligands) to optimize ligand–target interactions [33,34]. The optimal interaction is difficult to predict, as demonstrated in the study of Lindner *et al*. who examined the binding avidity of peptide-based MMIAs targeting the gastrin-releasing peptide receptor (GRPR) [33]. The effect of different valencies (n = 1, 2, 4, or 8) using poly(amidoamine) (PAMAM) dendrons and different polyethylene glycol (PEG) linker lengths was explored [33]. It was found that the dimer (n = 2) with three repeating units of ethylene glycol had the highest avidity. The authors concluded that the improved binding of the dimeric ligand (n = 2) in binding to its target is a consequence of a binding–rebinding effect rather than of the high local concentration of multivalent compounds [33]. The monomer showed a relatively constant binding affinity regardless of linker length. Interestingly, the tetra- and octavalent MMIAs had lower avidities, and even showed decreasing avidity with increasing linker length [33]. In the following we elaborate on three key factors: ligand–target interaction, linker length, and multivalency.

Ligand–Target Interaction

Medical imaging requires the best possible interaction between the naturally occurring target and the synthetic ligand to ensure that the physician can obtain the desired diagnostic information [27,29]. Therefore, it is important to select the correct target that allows multivalent binding of a specific ligand. Ideally, this ligand should contain an attachment point for the linker/core of the IA that does not interfere with ligand binding to the target [13]. In addition, one must choose whether the MMIA is a homo- or heteromultimer [29,98] and thus contains ligands for one or more targets, respectively [35], particularly because heteromultimers can generate a lower K_d^{multi} than homomultimers [29,98,99]. However, this is not a general solution, and depends on the diagnostic question. For example, a heteromultimer targets multiple biomarkers in the diseased tissue and therefore cannot provide information about a specific target [36], and homomultimers should be used if information is required for a specific target. However, heteromultimers are attractive if the expression levels of multiple targets in the same tissue change in a similar direction, as has been shown in tumors (e.g., integrin and gastrin-releasing peptide receptors: ^{18}F-labeled heterodimer binding to integrin $\alpha_V\beta_3$ and bombesin [37]) and potentially for neurodegenerative diseases (e.g., dopamine, histamine, and serotonin receptors).

The Nature of Multivalent Scaffolds

The ideal multivalent scaffold was originally defined as a multivalent scaffold that matches B_{max} by achieving $m = n = i$ [27]. However, studies on the PK of MMIAs demonstrate that other factors are important for achieving a high BP, because geometry and selectivity can determine the binding avidity [29], and this is dependent on Ω_i and on linker length [27]. In addition, quantification of MMIA valency and ligand–target contacts/interactions for higher-valent MMIAs remains challenging [38,39]. Nevertheless, when designing a new MMIA, it remains important to predefine the intended valency (n) of the final MMIA because this influences the choice of scaffold. For example, non-covalent liposomal MMIAs (whose preparation is primarily based on traditional benchmarks rather than on rational design approaches [40]) have a relatively random ligand density at their surface that is difficult to measure. However, there has been recent progress in determining the effective valency of these structures [41]. Therefore, tunable valency is easier to achieve by using covalent scaffolds, but they do not always lead to successful binding (Figure 2).

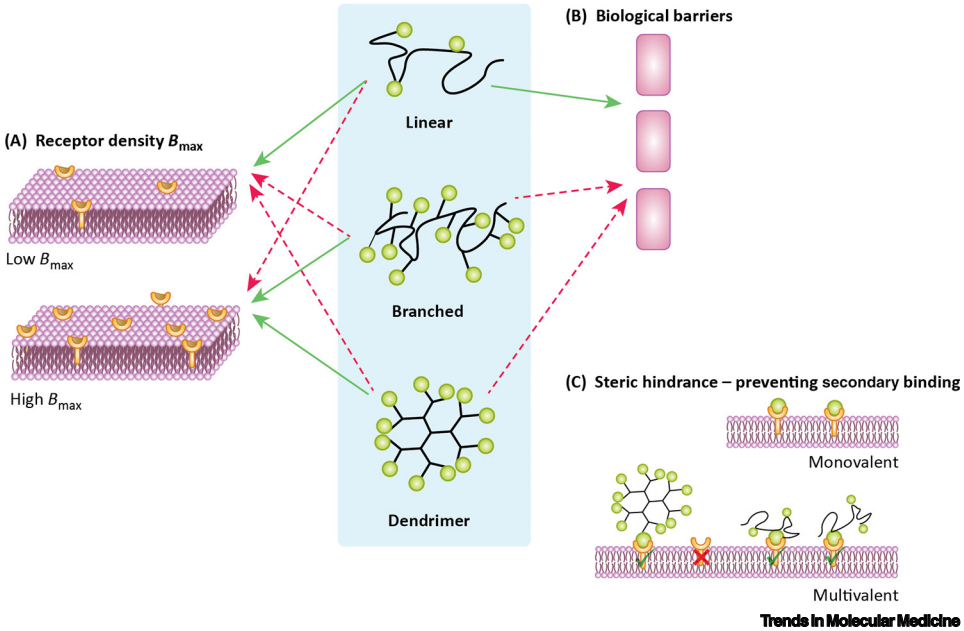

Figure 2. Representation of the Three Different Multivalent Scaffolds. The scaffolds (linear, branched, and dendritic constructs) are highlighted in the blue box and their beneficial (green solid arrows) or ineffective (red broken arrows) properties under some circumstances are illustrated. Linear polymers are the best option for targeting receptors with a low density (A) because they can form simultaneous target interactions even at larger distances. For high receptor density (A), globular dendrimers might be a better option because these branched polymers have tunable size and functionality. However, their large hydrodynamic radius hinders their penetration through several biological barriers (B), such as the tight junctions of the blood–brain barrier, mucus barriers, the blood–testis barrier, and glomerular filtration for renal clearance, and they also have greater plasma exposure [62]; in addition, their large radius can also result in steric hindrance at the target site, thus preventing a possible second multivalent molecular imaging agent (MMIA) from binding [48], whereas monovalent imaging agents (IAs) can more easily bind next to each other owing to their smaller size (C).

Linker Rigidity and Length

As noted earlier, the length of the linker plays an important role in maximizing Ω_i [27], and linker chemical composition and rigidity/flexibility also influence the interaction between ligand and target [29]. Linkers that are too long can decrease the binding avidity, and binding affinity assays showed a higher inhibitory constant (IC_{50}) for longer linkers independently of the valency of the multimer [33]. In addition, linkers that are too short do not allow simultaneous binding [29]. Furthermore, rigid linkers provide a fixed geometry whereas flexible linkers do not, and hence have a larger influence on the Ω_i [42]. The high entropy of flexible linkers can also strengthen the key interactions between ligand and target that decrease the K_d [29].

PK Properties Influence Image Quality

In addition to the interaction of MMIAs with molecular targets, their performance is also related to their PK properties. Whereas low molecular weight IAs show several nonspecific binding effects, short circulation times, and fast metabolism [43], MMIAs suffer from nonspecific tissue accumulation as a result of protein binding and prolonged circulation time, and their biodistribution differs from that of monovalent IAs [44,45]. An overview of some factors affecting biodistribution is given in Box 3. The topology of the MMIA mainly determines its distribution profile *in vivo* [46]. The circulation times of dendrimer-based or branched MMIAs are longer than for linear compounds, and the circulation time is dependent on the degree of branching [47]. Although these effects have been investigated in the field of drug delivery, they are also seen for MMIAs. Summer *et al.* investigated the protein binding and circulation of mono-, di-, and trivalent MMIAs targeting the

cholecystokinin 2 receptor [48]. Protein binding was found to depend on the valency: the monomer had the lowest percent protein binding (<5% after 4 h) whereas the trimer had the highest (~50% after 4 h) [48]. In addition, valency also governed circulation time, and the trimer showed highest tumor uptake at 4 h post-injection (p.i.) compared with 1 h p.i. for the monomer [48]. The same group also found that the trimer had a higher metabolic stability than either the dimer or the monomer, which explains their high targeting efficacy despite a prolonged circulation time [48].

Other Factors Influencing the BP of MMIAs

Solubility Effects Influence Efficiency

A confounding factor that accompanies the high molecular weight of MMIAs is their insolubility under physiological conditions. Babič *et al.* studied the imaging of diabetes mellitus by targeting the sulfonylurea receptor subtype 1 with the specific ligand glibenclamide, which is characterized by low cellular uptake [49]. Multimerization of glibenclamide was found to improve cellular uptake, and the fifth-generation PAMAM dendrimer core with 15 lipophilic glibenclamide ligands (n = 15) was the strongest binder. However, it had reduced solubility in aqueous media, and it was necessary to use a binder with five ligands (which displayed lower avidity) for *in vivo* studies [49]. Insoluble MMIAs cannot be adsorbed by the body and have low bioavailability [50]. The field of drug delivery already defined in 1975 that a successful multivalent nanosystem should include a solubilizing agent in addition to the multivalent scaffold, linker, and targeting moiety [43,51].

Preparation of MMIAs and Quantification of Ligand Density

The final number of ligands at the MMIA surface is a key parameter because ligand concentration and MMIA geometry determine the Ω_i. However, MMIA synthesis faces several challenges that influence successful ligand coupling. Starting from the core, the synthesis of a multivalent scaffold typically results in ligands being normally distributed on the MMIA surface [52]. Furthermore, peptide ligands are prone to denaturation during MMIA purification because of the use of organic solvents (e.g., acetonitrile), or can interact with the stationary phase used for chromatography [53]. This affects the amount of intact peptide ligand at the MMIA surface and thus its BP. It is therefore necessary to quantify the final ligand concentration at the MMIA surface. However, even with a good quantification method, the number of ligands available at the surface is not always exactly known because of ligand interactions with excessively flexible linkers [53,54], that can also reduce the avidity of the MMIA for the target site [55].

Box 3. The Fate of Molecular IAs on Their Journey through the Body

In the following we overview some factors that influence the binding of IAs and their PK. Because MMIAs belong to the class of pharmaceuticals, their *in vivo* behavior is governed by their administration, distribution, metabolism, and excretion (ADME) [43] profile (Figure I).

Administration

Most molecular IAs are injected intravenously [83–85] to make them immediately bioavailable [43]. However, there are some exceptions, including optical IAs that need to be applied topically for endoscopic applications [6] or orally, as recently shown in a study on the development of near-IR IAs [86].

Distribution

Because MMIAs specifically bind to a biomarker in the target tissue, their main challenge is to arrive at the target as an intact molecule. IAs can undergo site-specific extravasation followed by binding to the cell membrane and cellular uptake by transport or internalization [45]. However, cellular internalization, which is based on receptor-mediated endocytosis, might be altered when the valency of the MMIA is too high.

Metabolism and Excretion

MMIAs can form re-binding metabolites [55] which are unwelcome because they may hinder the binding of intact MMIAs and decrease their avidity, which results in a low binding potential of the MMIA. Therefore, MMIAs must be metabolically stable during the scan. Their subsequent metabolism and excretion is dependent on the composition and biodegradability of MMIAs [43], as well as on their size – different organs have specific clearance mechanisms and only compounds <5 nm can pass the glomerular filter of the kidneys for excretion into the urine [87]. This further depends on the type of multivalent scaffold because linear polymers can even pass through small pores owing to their high flexibility, and thus might still pass this filter [47,88] and thus be less potent in achieving high tumor accumulation [88].

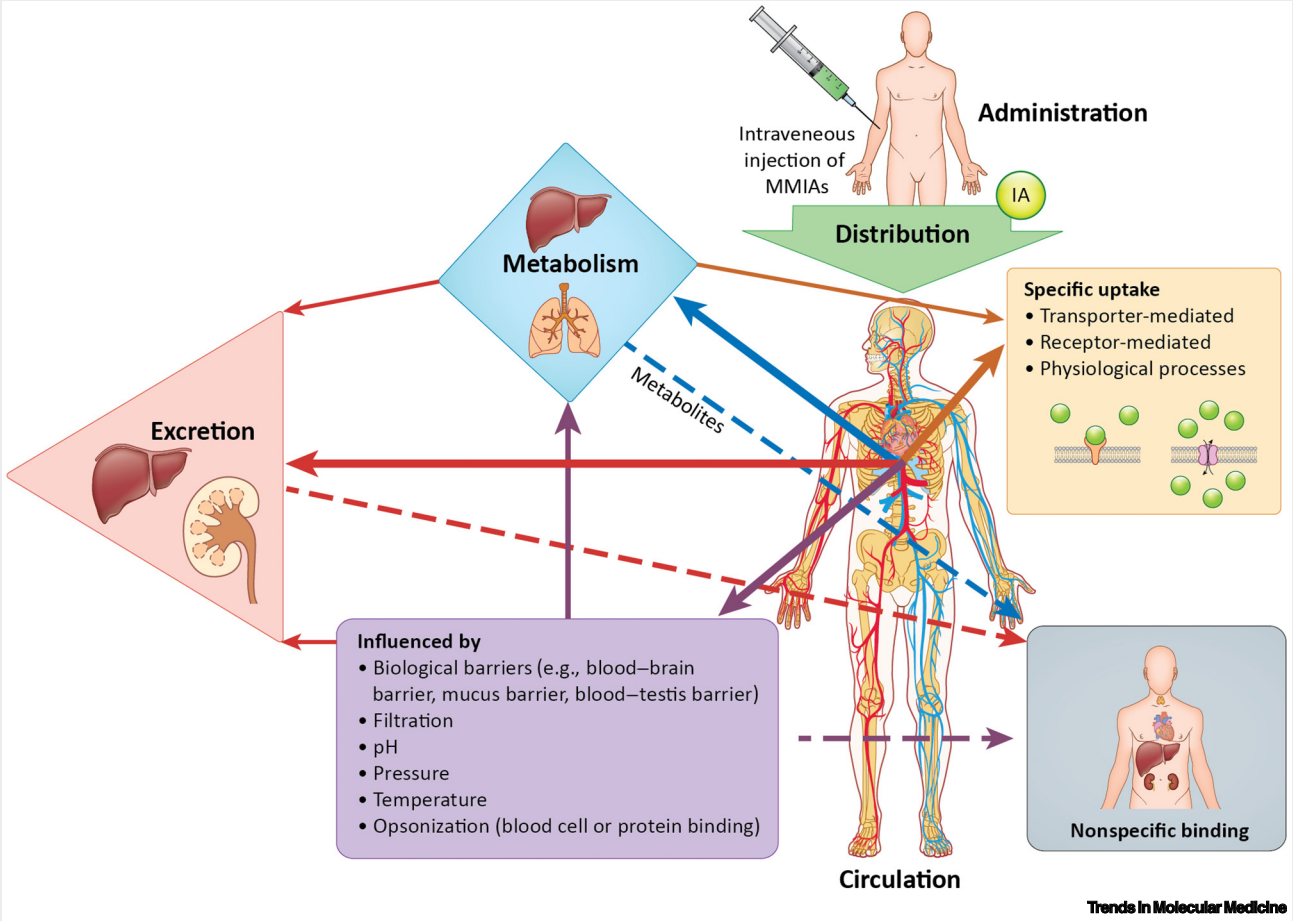

Figure I. Illustration of the Fate of Imaging Agents (IAs) Following Administration into the Human Body. Solid lines represent the normal fate of an IA in the body. Dashed lines represent confounding factors leading to nonspecific binding. The distribution of the IA depends on several factors. (i) Opsonization: the opsonization of blood plasma proteins towards IAs can result in clearance via the mononuclear phagocyte system (MPS) and might lead to reduced affinity for the target [45]. (ii) Nonspecific binding: this can be a consequence of opsonization or of physiological effects such as the enhanced permeation and retention (EPR) effect [45] and enzymatic degradation [89]. (iii) Hemorheology: blood vessel fluid dynamics influence the circulation time of IAs depending on the size, geometry, charge, and flexibility of the IA: liposomes tend to float in the 'cell-free layer' near to the blood vessel wall [45]. (iv) Disease-specific properties: several diseased tissues have specific properties; for example, tumors have high intratumoral pressure that is related to the EPR effect as well as to angiogenesis [45], and also have an altered pH [59]. These factors can influence the integrity of the multivalent molecular imaging agent (MMIA) because protonable groups within the MMIA can cause swelling of the constructs [45].

Biodegradation of MMIAs

Biodegradable multivalent scaffolds that enable controlled drug release are often employed in targeted drug delivery systems [56,57]. Although release takes place over a timescale of several hours to days, MMIAs show a prolonged circulation time and engineered degradation might be advantageous. Indeed, in some cases engineered degradation can result in activation of the imaging tag. For example, self-assembled MMIAs can quench fluorescent tags located in the core of the nanoparticle, but these can become fluorescent again following disassembly as a result of protein–RNA binding or a pH change [58]. A recent study exploited the altered pH of tumor tissues to selectively release super-paramagnetic iron oxide nanoparticles for MRI following endosomal initialization [59].

Translation to the Clinic

Despite several recent preclinical studies (Table 1), the translation of MMIAs to the clinic remains limited because of their specific properties (Box 4), including their prolonged circulation times and strict safety regulations [60]. Furthermore, extensive toxicity studies are required for each component of the MMIA [60], which is both costly and time-consuming. Multimers may not be suitable for all imaging techniques and pathophysiologies. Because of their prolonged circulation time, MMIAs are of limited utility for PET imaging because this is predominantly based on the radioactive decay of short-living radionuclides such as carbon-11 [**half-life** ($t_{1/2}$) of 20.4 minutes, >99% β^+] and gallium-68 ($t_{1/2}$ 67.9 minutes, 89% β^+) [61]. MMIAs will require longer-living radionuclides such as fluorine-18 ($t_{1/2}$ of 109.8 minutes, 97% β^+) [61] or zirconium-89 ($t_{1/2}$ of 78.4 days, 22.7% β^+) [61], and pre-targeting approaches might be a useful alternative that would permit successful PET imaging with MMIAs.

A Stepwise Approach to the Design of MMIAs

After identifying the challenges, we conclude that multivalency is not (yet) an established solution for increasing the avidity of IAs in clinical applications. We therefore recommend the following design steps that might assist in the design of future MMIAs for successful clinical translation.

Table 1. Selected Preclinical Studies Utilizing MMIAs[a]

Application	Target	Ligand	Valency	Core	Linker	Outcome	Refs
PET	Vascular endothelial growth factor receptor 2	**Vandetanib**	2	2,2′,2″-Nitrilo-*tris* (ethane-2,1-diyl)-*tris* (1H-imidazole-1-carboxylate)	N.A.	Higher tumor uptake of the dimer	[90]
OI and photoacoustic	Tumor	cRGD	Self-assembly	Silica-coated triblock copolymers	PEG	The cRGD-targeted MMIA showed higher tumor and spleen uptake, but lower uptake in non-targeted organs	[91]
SPECT	Folate receptor	Folic acid	1, 2, and 4	2-Hydrazinonicotinic acid and click with tricine and trisodium triphenylphosphine-3,3', 3''-trisulfonate	PEG	Monomer showed the highest uptake (after 4 h), followed by dimer	[34]
PET	Neurotensin receptor	Nlys8–Lys9–Pro10–Tyr11–Tle12–Leu13–OH (NT4)	3	1,4,7-Triazacyclononane-1,4,7-*tris*[(2-carboxyethyl) methylenephosphinic acid] (TRAP)	N.A.	Tumor uptake of monomer and trimer was in the same range, but the trimer showed slightly higher nonspecific binding	[92]
OI	Tumor	*N*-glycans		Polylysine	Six different copolymers	No valency mentioned in the article; the figure represents 16 ligands on the surface	[93]
PET	Prostate cancer	PESIN	1, 2, 4, and 8	PAMAM dendrimer	PEG	The dimer with a triethylene glycol linker has the lowest binding affinity and an improved biodistribution profile	[33]

[a]Abbreviations: cRGD, cyclic(Arg–Gly–Asp); N.A., not available; PAMAM, polyamido amine; PEG, polyethylene glycol; PESIN, peptide Pro–Glu–Ser–Ile–Asn.

Box 4. Clinical Trials of MMIAs

Only a few MMIAs have so far been evaluated in humans. In 2011, a fluorine-18 radiotracer utilizing a dimeric RGD peptide, [^{18}F]FPPRGD2, was tested for targeting $\alpha_v\beta_3$-integrins [94]. Initial PK and dosimetric studies were conducted in five healthy volunteers over a time-frame of 3 h, revealing fast renal clearance and relatively low liver uptake compared with another RGD-based radiotracer, [^{18}F]fluciatide [94]. A follow-up study of this dimeric homomultimer was published 3 years later in which eight breast cancer patients were scanned with [^{18}F]FPPRGD2 and compared with radiolabeled deoxyglucose [^{18}F]FDG [95].

Another trial was reported in 2014 in which a nanoparticle for PET-OI was evaluated for the detection of metastatic melanoma. The probe was constructed from a Cornell silica dot (C dot) and was functionalized with cyclic (c)-RGDY peptides and radiolabeled with iodine-124 ($t_{1/2}$ 100.2 minutes [61]) to form [^{124}I]cRGDY-PEG-C dots with a final size of 6–7 nm for the visualization of integrin-expressing cancers [73]. The PK of [^{124}I]cRGDY-PEG-C dots were studied for 72 h p.i. by measuring whole-body PET/computerized tomography scans after 2, 4, 24, and 72 h [73]. The MMIAs were not optimized for tumor detection, and were not able to detect tumor lesions, but showed fast renal clearance with an initial half-life of 3.57 h [73]. Radio-thin-layer-chromatography confirmed the integrity of the MMIA in blood for the first 24 h, but revealed metabolite formation in urine caused by enzymatic dehalogenation of iodine-124 [73].

Although both the examples mentioned above studied homomultimers, the first use of a heterodimer in humans was reported in 2016 for PET imaging. The radiotracer was designed to target both $\alpha_v\beta$ and gastrin-releasing peptide receptors (GRPRs) with the aim of prostate cancer imaging using [^{68}Ga]BBN-RGD [96] because bombesin (BBN) derivatives bind selectively to GRPR. This first-in-human study was performed in five healthy volunteers and 13 patients with prostate cancer [96]. For validation of the tracer, a follow-up scan using [^{68}Ga]NOTA-Aca-BBN$_{7-14}$ was performed [96,97]. In this study, [^{68}Ga]BBN-RGD detected one more primary prostate cancer lesion than [^{68}Ga]NOTA-Aca-BBN$_{7-14}$, which was in agreement with biopsy immunohistochemistry [96] because one lesion was GRPR negative [96]. An additional MRI scan could detect all lymph nodes, whereas [^{68}Ga]BBN-RGD was able to detect more bone metastases than MRI and [^{68}Ga]BBN alone, demonstrating that the heterodimer can indeed be advantageous in detecting more lesions [96].

(i) Select the Target and the Ligand

The first step is to define the best possible ligand that shows the strongest binding interactions with the target, generally a disease-specific biomarker. The point of attachment to the multivalent core or imaging tag should not affect the binding of the ligand to the target. However, because this might not always be the case, structure–activity relationships can be used to predetermine the positions that exhibit the lowest interference with the key interactions. In addition, a choice must be made between homo- and hetero-multivalency [13,29].

(ii) Determine the Target Density

For optimal binding of MMIAs, the degeneracy coefficient Ω_i needs to be maximized. The density and average distances of the targets should be determined to choose the right ligand with appropriate linker length.

(iii) Select the Most Suitable Multivalent Scaffold and Appropriate Linker Length

The multivalent scaffold is of importance because it can improve the properties of the MMIA in terms of circulation time, solubility, and immunogenicity [62]. Ideally, the ligand concentration is optimized to the target concentration by adjusting the linker length to reduce steric hindrance at the target site [35]. In addition, the multivalent scaffold should not only be biocompatible but ideally also be biodegradable, with degradation times that suit the imaging modality and support the optimal circulation time of the MMIA.

(iv) Consider Biological Barriers When Choosing the Appropriate MMIA

The human body features several protective barriers, some of which may need to be crossed to reach the target. For imaging cancer vascularization, the intertumoral pH

and the pressure gradient are the main obstacles [45]. Brain imaging requires passage of the blood–brain barrier (BBB) that is highly impermeable owing to tight junctions associated with neurovascular units [13,63,64]. To date there is no generic solution to all the biological hurdles that an MMIA will encounter. Intrathecal injection to circumvent BBB passage has been successfully investigated [65], but requires highly trained personnel and includes additional requirements regarding the formulation of the MMIA, for example, the absence of organic solvents. The most important factors that need to be considered are possible increased opsonization effects resulting in nonspecific binding.

(v) Select the Properties of the Linker

The linker has a high impact on the avidity of ligands [66]. PEG-based linkers are one of the first choices because PEG copolymers are water-soluble, neutrally charged, and biocompatible, and have properties that shield them from degradation and excretion [62]. However, PEGylation also favors nonspecific binding of MMIAs, which lowers the remaining fraction of MMIAs that can target the diseased tissue [67].

(vi) Define the Method for MMIA Synthesis

The quantification of ligands at the MMIA surface is of great importance because only surface ligands can participate in the multivalency effect. Therefore, the optimal method of synthesis should enable full control of the ligand concentration through convergent or bottom-up approaches [52,68] in which the ligand is first attached to the linker and then coupled to the multivalent scaffold.

(vii) Predetermine the Important Properties of the MMIA *in Vitro*

During the development of MMIAs, specific features should be assessed *in vitro*. Because MMIAs are more likely to be toxic than small monovalent molecules, they should be tested for cytotoxicity as well as for binding affinity and specific binding. In addition, nonspecific protein binding should be determined by structure–activity relationships or surface plasmon resonance following incubation with blood plasma proteins [53,69–71].

(viii) Study Target Binding and PK *in Vivo*

Before the first clinical trials, extensive preclinical *in vivo* experiments must be conducted to determine the PK and metabolic stability of the MMIA. The complex biological and physiological interactions within the body cannot yet be predicted, and extensive evaluation in animals is necessary before further translation towards human studies. Pharmacodynamic (PD)/PK studies are essential to determine the potential imaging efficiency of a new MMIA.

(ix) Safety Assessment

Applications in humans require accurate safety assessment. Because several aspects differ between mono- and multivalent IAs, different assessment methods are necessary. Usually, novel IAs need to be investigated for *in vivo* toxicity according to ICH (International Council for Harmonization of Technical Requirements for Pharmaceuticals for Human Use) guidelines M3 (R2) [72]. These toxicity studies require several hundreds of milligrams of compounds, and this is often not possible for MMIAs. Alternatively, the toxicities of the individual components (core, linker, monomer) may be assessed.

Clinician's Corner

The imaging efficacy of molecular imaging agents can be problematic when the density of the target (B_{max}) is too low and the administered imaging agents have poor binding affinity (high K_d) or are not sufficiently metabolically stable to accumulate at the target in adequate amounts. In these cases, the image contrast, which is measured as the BP (defined as the B_{max}:K_d ratio), is too low to obtain a diagnostic image. Multivalent molecular imaging agents can be used to increase the binding affinity (lower K_d) to improve the BP and thus the imaging contrast.

Multivalent imaging agents can increase binding efficacy and can be an alternative to the existing, but often nonideal, imaging agents that are already used in the clinic. Several publications report improved imaging contrast by the application of multivalency in preclinical settings.

The main obstacles to the development of multivalent imaging agents are (i) the lack of understanding of how to design agents to obtain the desired avidity and PK, and (ii) expensive toxicity studies – because multivalent imaging agents are significantly larger molecules than common monovalent imaging agents.

Multivalent imaging agents would offer great benefit for the diagnosis of pathophysiology involving changes in the expression or function of biological targets such as enzymes, antigens, and receptors. Multivalent imaging agents can also be used to explore novel drug targets.

(x) Good Manufacturing Practice (GMP) Production

The production of MMIAs for clinical studies requires compliance with GMP. MMIAs differ from monovalent IAs in that the molecular structure of the multivalent analog is often less precisely defined, and appropriate analytical methods are necessary to demonstrate the quality of the MMIAs.

Outstanding Questions

For which clinical applications will MMIAs bring medical imaging to a higher level?

Do MMIAs have the potential to be a game-changer in clinical practice?

Do we need to benchmark multimodal IAs against current clinical IAs, and what criteria should be taken into consideration?

Which are the biggest challenges that need further investigation to overcome with respect to the informed design of MMIAs?

Which aspects need further research to develop and produce MMIAs in a cost-effective way?

Concluding Remarks

Although numerous preclinical studies of MMIAs have been published, their routine application in clinical practice has not yet been achieved. We have provided an overview of the main challenges involved in translating multivalent imaging probes to the clinic. The main hurdles are the design of an appropriate multivalent system for the desired target, insolubility, protein binding, and the challenging characterization and quantification of the number of ligands. These aspects have a major impact on MMIA success in the (pre)clinical applications. However, the advantages of high avidity and the possibility of modulating their circulation time mean that MMIAs hold great potential, as revealed by clinical trials such as those for ^{124}I-cRGDY-PEG-C dots [73]. The design of MMIAs reviewed here does not yet encompass all obstacles and possible solutions, but it is intended as a starting point for understanding the complexity of multivalent IAs with a view to facilitating further exploration of their potential in clinical diagnostics (see Outstanding Questions).

Acknowledgments

The authors would like to thank the provinces Overijssel and Gelderland, the Functional Molecular System (FMS) Gravitation program, and the project consortium of the Center of Medical Imaging – North East Netherlands (CMI-NEN) for funding.

Supplemental Information

Supplemental information associated with this article can be found online at https://doi.org/10.1016/j.molmed.2020.12.006.

References

1. Bradley, D. and Bradley, K.E. (2002) The value of diagnostic medical imaging. *N. C. Med. J.* 75, 121–125
2. Morris, P. and Perkins, A. (2012) Optical imaging. *Lancet* 379, 1525–1533
3. Histed, S.N. *et al.* (2012) Review of functional/anatomic imaging in oncology. *Nucl. Med. Commun.* 33, 349–361
4. Willmann, J.K. *et al.* (2008) Molecular imaging in drug development. *Nat. Rev. Drug Discov.* 7, 591–607
5. James, M.L. and Gambhir, S.S. (2012) A molecular imaging primer: modalities, imaging agents and applications. *Physiol. Rev.* 92, 897–965
6. Seaman, M.E. *et al.* (2010) Molecular imaging agents: impact on diagnosis and therapeutics in oncology. *Expert Rev. Mol. Med.* 12, E20
7. Cassidy, P.J. and Radda, G.K. (2005) Molecular imaging perspectives. *J. R. Soc. Interface* 2, 133–144
8. Miller, J.C. and Thrall, J.H. (2004) Clinical molecular imaging. *J. Am. Coll. Radiol.* 1, 4–23
9. Gallagher, F.A. (2010) An introduction to functional and molecular imaging with MRI. *Clin. Radiol.* 65, 557–566
10. Arsiwala, A. *et al.* (2019) Designing multivalent ligands to control biological interactions: from vaccines and cellular effectors to targeted drug delivery. *Chem. Asian J.* 14, 244–255
11. Kiessling, L.L. *et al.* (2000) Synthetic multivalent ligands in the exploration of cell-surface interactions. *Curr. Opin. Chem. Biol.* 4, 696–703
12. Agdeppa, E.D. and Spilker, M.E. (2009) A review of imaging agent development. *AAPS J.* 11, 286–299
13. Elsinga, P.H. (2002) Radiopharmaceutical chemistry for positron emission tomography. *Methods* 27, 208–217
14. Pike, V.W. (2009) PET radiotracers: crossing the blood–brain barrier and surviving metabolism. *Trends Pharmacol. Sci.* 30, 431–440
15. Zhang, Y. and Fox, G.B. (2012) PET imaging for receptor occupancy: meditations on calculation and simplification. *J. Biomed. Res.* 26, 69–76
16. Huang, Z. *et al.* (2008) Misdiagnoses of ^{11}C-choline combined with ^{18}F-FDG PET imaging in brain tumors. *Nucl. Med. Commun.* 29, 354–358
17. Mammen, M. *et al.* (1998) Polyvalent interactions in biological systems: implications for design and use of multivalent ligands and inhibitors. *Angew. Chem. Int. Ed. Engl.* 37, 2754–2794
18. Bhatia, S. *et al.* (2016) Pathogen inhibition by multivalent ligand architectures. *J. Am. Chem. Soc.* 138, 8654–8666
19. Klimovich, V.B. (2011) IgM and its receptors: structural and functional aspects. *Biochem. Mosc.* 76, 534–549
20. Rudnick, S.I. and Adams, G.P. (2009) Affinity and avidity in antibody-based tumor targeting. *Cancer Biother. Radiopharm.* 24, 155–161
21. Welsh, D.J. and Smith, D.K. (2011) Comparing dendritic and self-assembly strategies to multivalency-RGD peptide–integrin interaction. *Org. Biomol. Chem.* 9, 4795–4801
22. Errington, W.J. *et al.* (2019) Mechanisms of noncanonical binding dynamics in multivalent protein–protein interactions. *PNAS* 116, 25659–25667
23. Rosca, E.V. *et al.* (2007) Specificity and mobility of biomacromolecular, multivalent constructs for cellular targeting. *Biomacromolecules* 8, 3830–3835
24. Caplan, M.R. and Rosca, E.V. (2005) Targeting drugs to combinations of receptors: a modeling analysis of potential specificity. *Ann. Biomed. Eng.* 33, 1113–1124
25. Claveria-Gimeno, R. *et al.* (2017) A look at ligand binding thermodynamics in drug Discovery. *Expert Opin. Drug Discov.* 12, 363–377
26. Borroto-Escuela, D.O. and Fuxe, K. (2019) Oligomeric receptor complexes and their allosteric receptor–receptor interactions in

the plasma membrane represents a new biological principle for integration of signals in the CNS. *Front. Mol. Neurosci.* 12, 230
27. Tjandra, K.C. and Thordarson, P. (2019) Multivalency in drug delivery – when is it too much of a good thing? *Bioconjug. Chem.* 30, 503–514
28. Gestwicki, J.E. *et al.* (2002) Influencing receptor–ligand binding mechanisms with multivalent ligand architecture. *J. Am. Chem. Soc.* 124, 14922–14933
29. Carlucci, G. *et al.* (2012) Multimerization improves targeting of peptide radio-pharmaceuticals. *Curr. Pharm. Des.* 18, 2501–2516
30. Debbage, P. and Jaschke, W. (2018) Molecular imaging with nanoparticles: giant roles for dwarf actors. *Histochem. Cell Biol.* 130, 845–875
31. Xia, Y. *et al.* (2019) Liposome-based probes for molecular imaging: from basic research to the bedside. *Nanoscale* 11, 5822–5838
32. Petersen, A.L. *et al.* (2012) Liposome imaging agents in personalized medicine. *Adv. Drug Deliv. Rev.* 64, 1417–1435
33. Lindner, S. *et al.* (2014) PESIN multimerization improves receptor avidities and in vivo tumor targeting properties to GRPR-overexpressing tumours. *Bioconjug. Chem.* 25, 489–500
34. Guo, Z. *et al.* (2017) Development of a new FR-targeting agent ^{99m}Tc-HYNFA with improved imaging contrast and comparison of multimerization and/ or pegylation strategies for radio-folate modification. *Mol. Pharm.* 14, 3780–3788
35. Handl, H.L. *et al.* (2005) Hitting multiple targets with multimeric ligands. *Expert Opin. Ther. Targets* 8, 565–586
36. Bandari, R.P. *et al.* (2014) Synthesis and biological evaluation of copper-64 radiolabeled [DUPA-6-Ahx-(NODAGA)-5-Ava-BBN (7–14)NH_2], a novel bivalent targeting vector having affinity for a two distinct biomarkers (GRPR/PSMA) of prostate cancer. *Nucl. Med. Biol.* 41, 355–363
37. Li, Z.-B. *et al.* (2008) ^{18}F-labeled BBN–RGD heterodimer for prostate cancer imaging. *J. Nucl. Med.* 49, 453–461
38. Lin, J. *et al.* (2018) Quantification of multivalency in protein-oligomer-coated nanoparticles targeting dynamic membrane glycan receptors. *Langmuir* 34, 8415–8421
39. Horáček, M. *et al.* (2020) Dynamic single-molecule counting for the quantification and optimization pf nanoparticle functionalization protocols. *Nanoscale* 12, 4128–4136
40. Noble, G.T. *et al.* (2014) Ligand-targeted liposome design: challenges and fundamental considerations. *Trends Biotechnol.* 32, 32–45
41. Belfiore, L. *et al.* (2018) Quantification of ligand density and stoichiometry on the surface of liposomes using single-molecule fluorescence imaging. *J. Control. Release* 278, 80–86
42. Curk, T. *et al.* (2018) Design principles for super selectivity using multivalent interactions. In *Multivalency* (Huskens, J. *et al.*, eds), pp. 75–101, John Wiley & Sons
43. Markovsky, E. *et al.* (2012) Administration, distribution, metabolism and elimination of polymer therapeutics. *J. Control. Release* 161, 446–460
44. Cheng, L. *et al.* (2016) Dual-modality positron emission tomography/ optical image-guided photodynamic cancer therapy with chlorin e6-containing nanomicelles. *ACS Nano* 10, 7721–7730
45. Blanco, E. *et al.* (2015) Principles of nanoparticle design for overcoming biological barriers to drug delivery. *Nat. Biotechnol.* 33, 941–951
46. Nasongkla, N. *et al.* (2009) Dependence of pharmacokinetics and biodistribution on polymer architecture: effect of cyclic versus linear polymers. *J. Am. Chem. Soc.* 131, 3842–3843
47. Lee, C.C. *et al.* (2005) Designing dendrimers for biological applications. *Nat. Biotechnol.* 23, 1517–1526
48. Summer, D. *et al.* (2018) Exploiting the concept of multivalency with ^{68}Ga- and ^{89}Zr-labelled fusarinine C-minigastrin bioconjugates for targeting CCK2R expression. *Contrast Media Mol. Imaging*, 3171794
49. Babič, A. *et al.* (2016) Multivalent glibenclamide to generate islet specific imaging probes. *Biomaterials* 75, 1–12
50. Savjani, K.T. *et al.* (2012) Drug solubility: importance and enhancement techniques. *ISRN Pharm.* 195727
51. Ringsdorf, H.J. (1975) Structure and properties of pharmacologically active polymers. *Polymer Sci.: Symposium* 51, 135–153
52. van Dongen, M.A. *et al.* (2014) Multivalent polymers for drug delivery and imaging: the callenges of conjugation. *Biomacromolecules* 15, 3215–3234
53. Sapsford, K.E. *et al.* (2011) Analyzing nanomaterial bioconjugates: a review of current and emerging purification and characterization techniques. *Anal. Chem.* 83, 4453–4488
54. Abstiens, K. (2019) Ligand density and linker length are critical factors for multivalent nanoparticle–receptor interactions. *ACS Appl. Mater. Interfaces* 11, 1311–1320
55. Summer, D. *et al.* (2018) Multimerization results in formation of re-bindable metabolites: a proof of concept study with FSC-based minigastrin imaging probes targeting CCK2R expression. *PLoS One* 13, e0201224
56. Uhrich, K.E. *et al.* (1995) Polymeric systems for controlled drug release. *Chem. Rev.* 99, 3181–3198
57. Ekkelenkamp, A.E. *et al.* (2018) Responsive crosslinked polymer nanogels for imaging and therapeutic delivery. *J. Mater. Chem. B* 2018, 210–235
58. Zhang, P. *et al.* (2015) Activatable nanoprobes for biomolecular detection. *Curr. Opin. Biotechnol.* 34, 171–179
59. Wan, L. *et al.* (2020) A novel intratumoral pH/redox-dual-responsive nanoplatform for cancer MR imaging and therapy. *J. Colloid Interface Sci.* 573, 263–277
60. Choyke, P.L. (2014) Nanoparticles: take only pictures, leave only footprints. *Sci. Transl. Med.* 6, 260fs44
61. Conti, M. and Eriksson, L. (2016) Physics on pure and non-pure positron emitters for PET: a review and a discussion. *EJNMMI Phys.* 3, 8
62. Ekladious, I. *et al.* (2018) Polymer-drug conjugate therapeutics: advances, insights and prospects. *Nat. Rev. Drug Discov.* 18, 273–294
63. Avsenik, J. *et al.* (2015) Blood–brain barrier permeability imaging using perfusion computed tomography. *Radiol. Oncol.* 49, 107–114
64. Grabrucker, A.M. *et al.* (2016) Nanoparticle transport across the blood brain barrier. *Tissue Barriers* 4, e1153568
65. Fowler, M.J. *et al.* (2020) Intrathecal drug delivery in the era of nanomedicine. *Adv. Drug Deliv. Rev.* 165–166, 77–95
66. Paolino, M. *et al.* (2014) Dendrimeric tetravalent ligands for the serotonin-gated ion channel. *Chem. Commun.* 50, 8582–8585
67. Bumbaca, B. *et al.* (2019) Pharmacokinetics of protein and peptide conjugates. *Drug Metab. Pharmacokinet.* 34, 42–54
68. Hawker, C.J. and Frechet, J.M.J. (1990) *J. Am. Chem. Soc.* 112, 7638–7647
69. Bucaite, G. *et al.* (2019) Interplay between affinity and valency in effector cell degranulation: a model system with procalcin allergens and human patient-derived IgE antibodies. *J. Immunol.* 203, 1693–1700
70. Lexa, K.W. *et al.* (2014) A structure-based model for predicting serum albumin binding. *PLoS One* 9, e93323
71. Fabini, E. and Danielson, U.H. (2017) Monitoring drug–serum protein interactions for early ADME prediction through surface plasmon resonance technology. *J. Pharm. Biomed. Anal.* 144, 188–194
72. European Medicines Agency (2008) ICH Topic M3: Non-Clinical Safety Studies for the Conduct of Human Clinical Trials and Marketing Authorization for Pharmaceuticals. (CMP/ICH/286/95). EMEA
73. Phillips, E. *et al.* (2014) Clinical translation of an ultrasmall inorganic optical-PET imaging nanoparticle probe. *Sci. Transl. Med.* 6, 260ra149
74. Hernot, S. *et al.* (2019) Latest developments in molecular tracers for fluorescence image-guided cancer surgery. *Lancet Oncol.* 20, e354–e367
75. Chen, K. and Chen, X. (2010) Design and development of molecular imaging probes. *Curr. Top. Med. Chem.* 10, 1227–1236
76. Turkheimer, F.E. *et al.* (2015) The methodology of TSPO imaging with positron emission tomography. *Biochem. Soc. Trans.* 43, 586–592
77. Meares, C.F. (2008) The chemistry of irreversible capture. *Adv. Drug Deliv. Rev.* 60, 1383–1388
78. Kopka, K. *et al.* (2003) Design of new β1-seletive adrenoceptor ligands as potential radioligands for in vivo imaging. *Bioorg. Med. Chem.* 11, 3513–3527
79. Ehrlich, P.H. (1979) The effect of multivalency on the specificity of protein and cell interactions. *J. Theor. Biol.* 81, 123–127

80. Kitov, P.I. and Bundle, D.R. (2003) On the nature of the multivalency effect: a thermodynamic model. *J. Am. Chem. Soc.* 125, 16271–16284
81. Sansone, F. and Casnati, A. (2013) Multivalent glycocalixarenes for recognition of biological macromolecules: glycocalyx mimics capable of multitasking. *Chem. Soc. Rev.* 42, 4623–4639
82. Tito, N.B. (2019) Multivalent 'attacker and guard' strategy for targeting surfaces with low receptor density. *J. Chem. Phys.* 150, 184907
83. Caldwell, J. *et al.* (1995) An introduction to drug disposition: the basic principles of absorption, distribution, metabolism, and excretion. *Toxicol. Pathol.* 23, 102–114
84. Joshi, B.P. and Wang, T.D. (2018) Targeted optical imaging agents in cancer: focus on clinical applications. *Contrast Media Mol. Imaging* 2018, 2015237
85. Cuggino, J.C. *et al.* (2019) Crossing biological barriers with nanogels to improve drug delivery performance. *J. Control. Release* 307, 221–246
86. Bhatnagar, S. *et al.* (2018) Oral administration and detection of a near-infrared molecular imaging agent in an orthotopic mouse model for breast cancer screening. *Mol. Pharm.* 15, 1746–1754
87. Thomas, O.S. and Weber, W. (2019) Overcoming physiological barriers to nanoparticle delivery – are we there yet? *Front. Bioeng. Biotechnol.* 7, 415
88. Chen, B. *et al.* (2009) The influence of polymer topology on pharmacokinetics: differences between cyclic and linear PEGylated poly (acrylic acid) comb polymers. *J Control Release* 140, 203–209
89. Dancy, J.C. *et al.* (2020) Decreased nonspecific adhesivity, receptor-targeted therapeutic nanoparticles for primary and metastatic breast cancer. *Sci. Adv.* 6, eaax3931
90. Li, F. *et al.* (2014) A tyrosine kinase inhibitor-based high-affinity PET radiopharmaceutical targets vascular endothelial growth factor receptor. *J. Nucl. Med.* 55, 1525–1531
91. Zhen, X. *et al.* (2017) Surface engineering of semiconducting polymer nanoparticles for amplified photoacoustic imaging. *Biomaterials* 127, 97–106
92. Maschauer, S. *et al.* (2017) Theranostic value of multimers: lessons learned from trimerization of neurotensin receptor ligands and other targeting vectors. *Pharmaceuticals* 10, 29
93. Ogura, A. *et al.* (2016) Glycan multivalency effects towards albumin enable N-glycan-dependent tumor targeting. Bioorganic Med. *Chem. Lett.* 26, 2251–2254
94. Mittra, E.S. *et al.* (2011) Pilot pharmacokinetic and dosimetric studies of 18F-FPPRGD2: a PET radiopharmaceutical agent for Imaging avβ3 integrin levels. *Radiology* 260, 182–191
95. Iagaru, A. *et al.* (2014) ^{18}F-FPPRGD2 PET/CT: pilot phase evaluation of breast cancer patients. *Radiology* 273, 549–559
96. Zhang, J. *et al.* (2017) Clinical translation of a dual integrin $\alpha_v\beta_3$- and gastrin-releasing peptide receptor-targeting PET radiotracer, ^{68}Ga–BBN–RGD. *J. Nucl. Med.* 58, 228–234
97. Zhang, J. *et al.* (2016) ^{68}Ga-NOTA-Aca-BBN(7–14) PET/CT in healthy volunteers and glioma patients. *J. Nucl. Med.* 57, 9–14
98. McKenzie, M. *et al.* (2018) Multivalent binding of a ligand-coated particle: role of shape, size, and ligand heterogeneity. *Biophys. J.* 114, 1830–1846
99. Eder, M. *et al.* (2014) Preclinical evaluation of a bispecific low-molecular heterodimer targeting both PSMA and GRPR for improved PET imaging and therapy of prostate cancer. *Prostate* 74, 659–668